Supplementary part A (S)

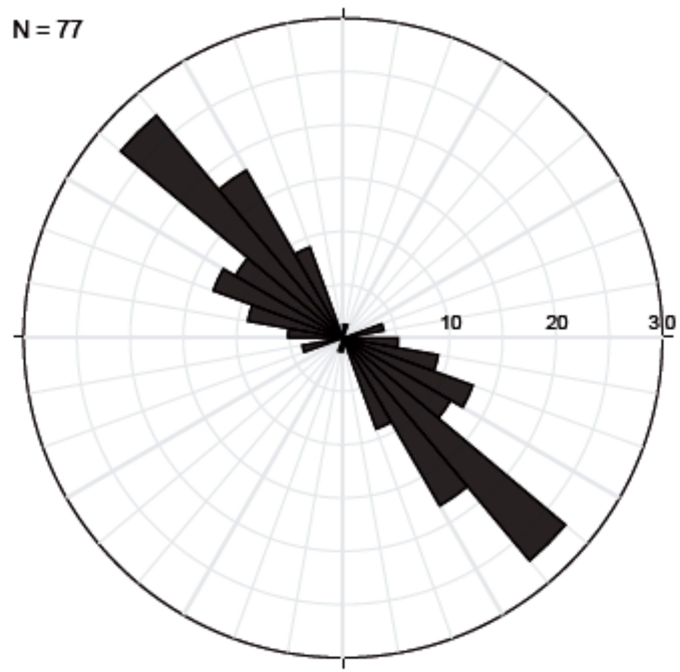

Figure 1S: Rose diagram for 77 faults mapped on the Geological Map of Tiwi .

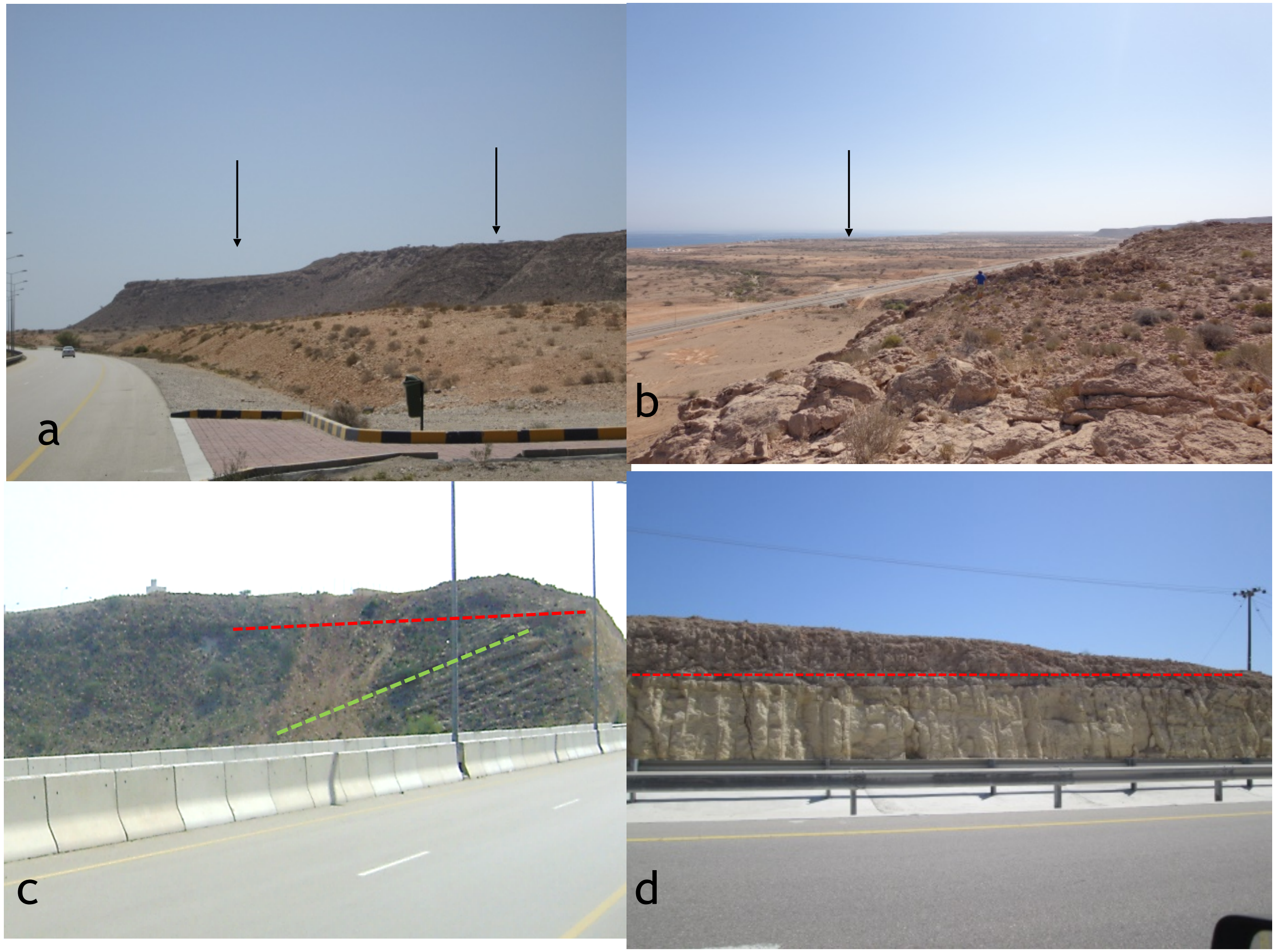

Figure 2S: a) Uplifted marine terraces of the study area. View is to the southeast towards Tiwi. Terrace 3 is marked by black arrows. The difference in elevation of the two arrows is because of perspective difference due distance b) Uplifted marine terraces of the study area. View is to southeast (The abrasion platform of terrace 2 is marked by black arrow). c) Angular unconformity between Neogene and Quaternary deposits in cross section. View is to southeast close to Dibbab. d) Unconformity between Neogene and Quaternary deposits in strike section. View is to the south towards the coastline.

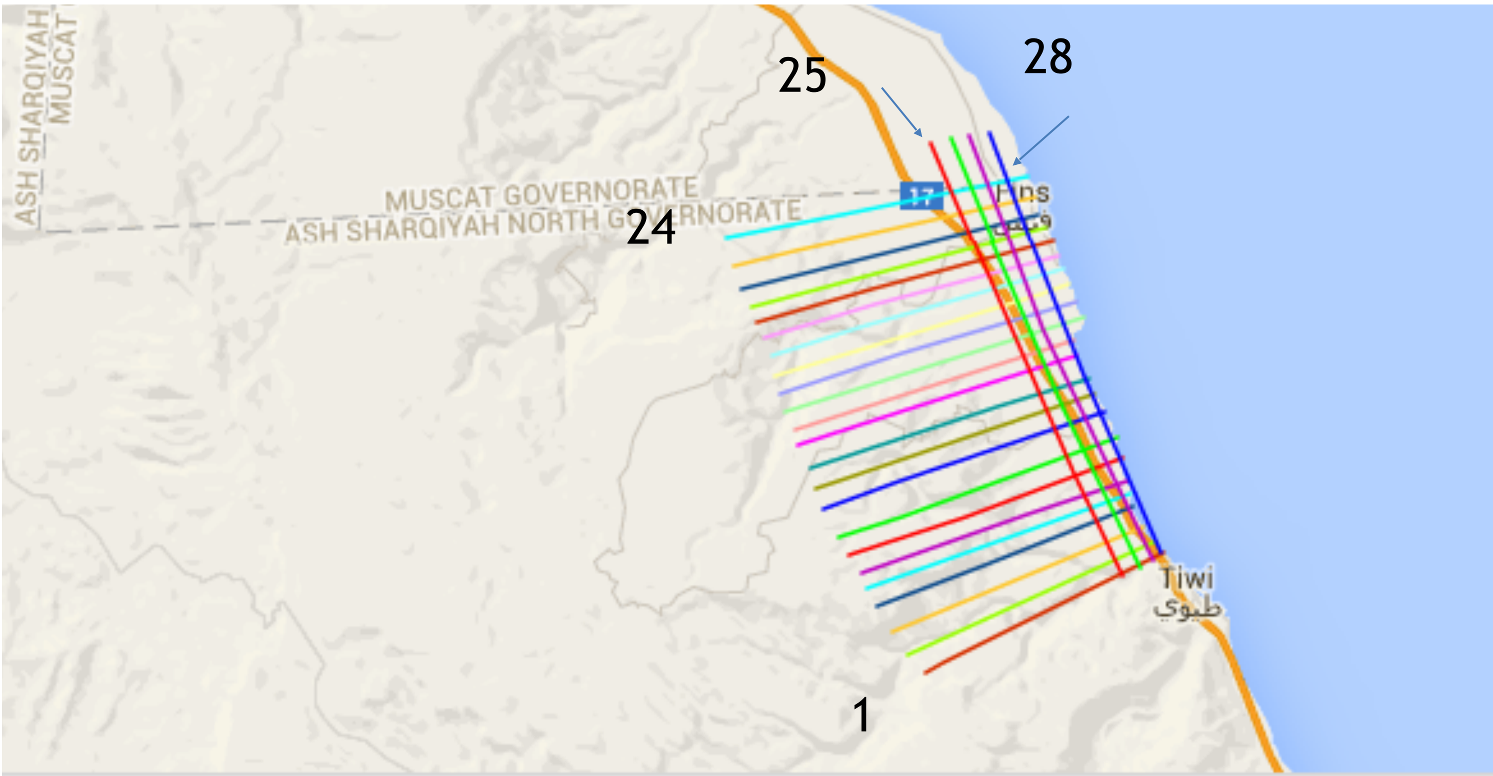

Figure 3S: Profiles 1-24 vertical to the coastline along Tiwi to Fins and 25-28 longitudinal profiles to the coastline. For the profiles Google earth engine was used (Google Earth Engine Team, 2015. Google Earth Engine: A planetary-scale geospatial analysis platform. https://earthengine.google.com)

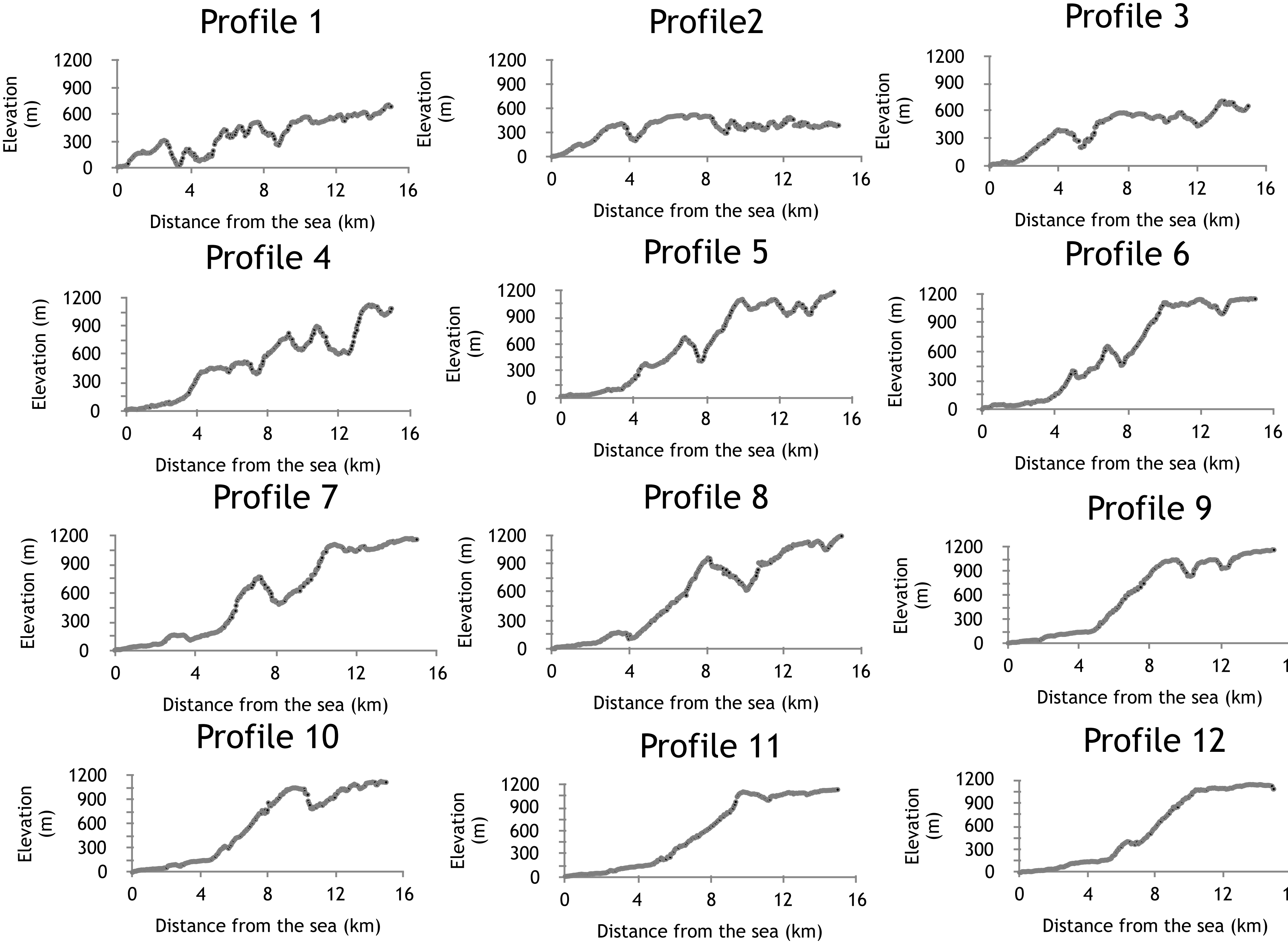

Figure 4Sa: Profiles 1-24 and correspond to those in Fig. 2SL

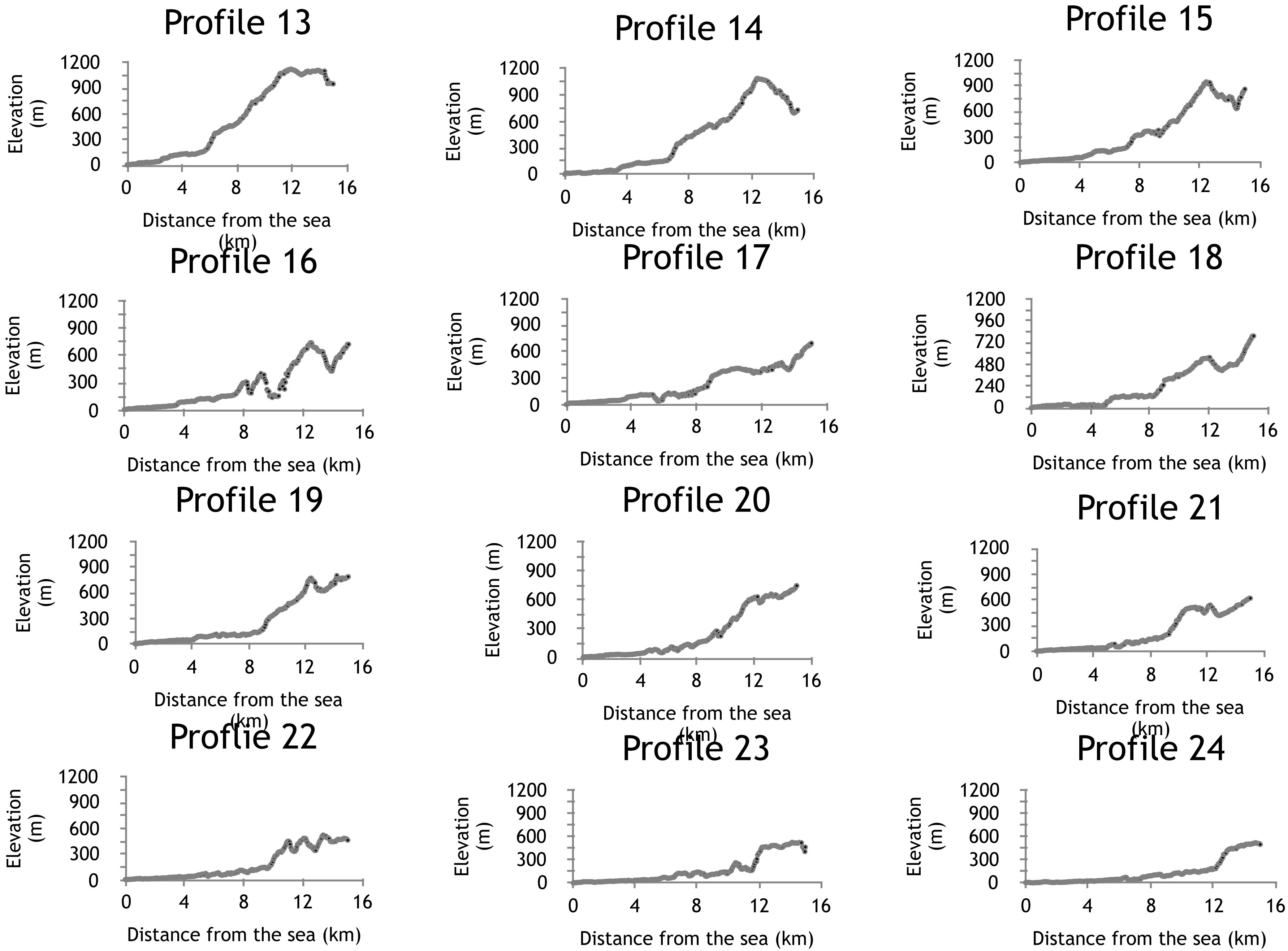

Figure 4Sa: Profiles 1-24 continues

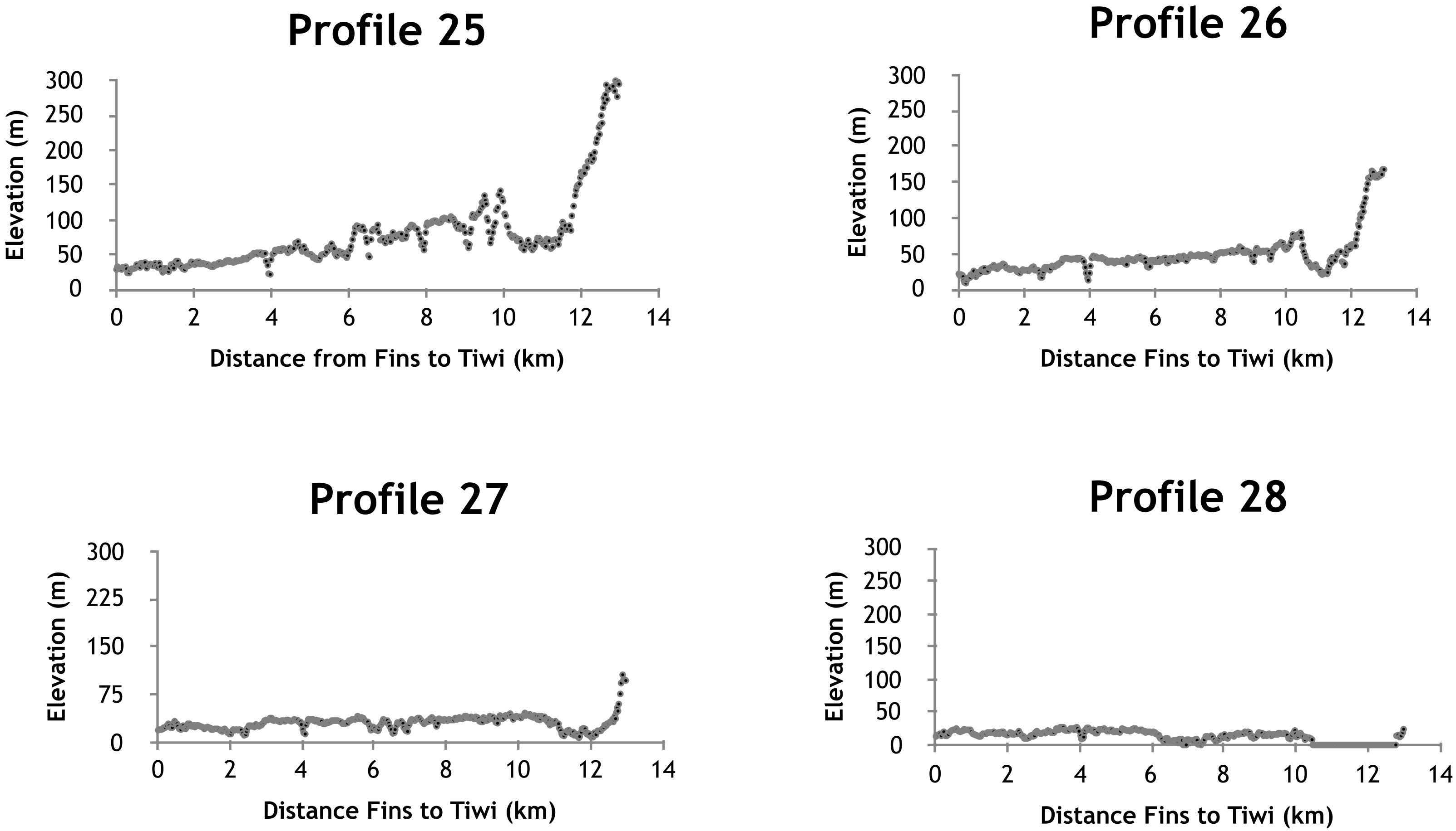

Figure 4Sb. Profiles 25-28 correspond to those in Fig. 2SL

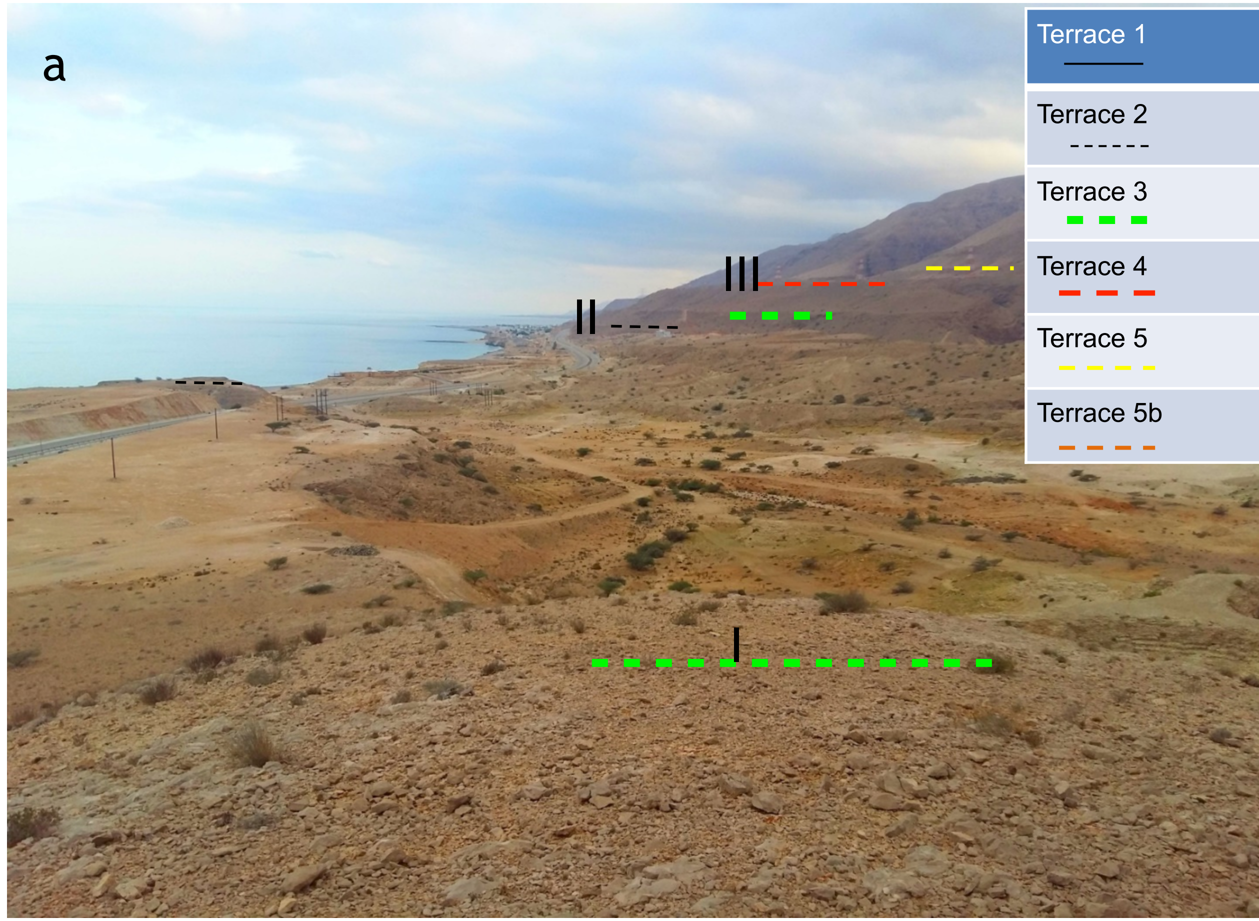

Figure 5S: a) Terraces 2-5 shot from point I. View is to the southeast. b) Terraces 4, 5 and 5b shot from point III. View is to the west. Colours correspond to Fig. 5. The wadi shown in 5Sb is Wadi Shab

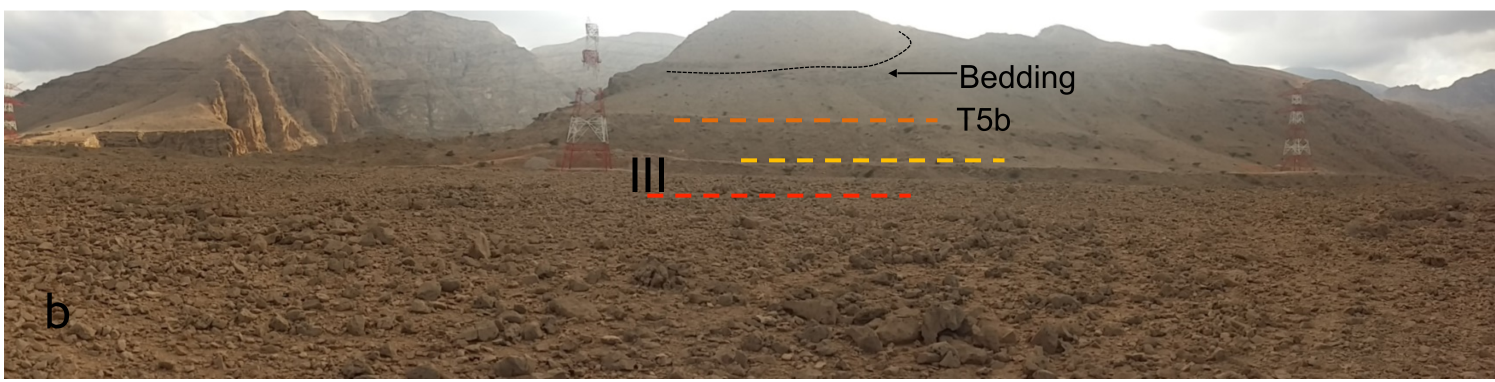

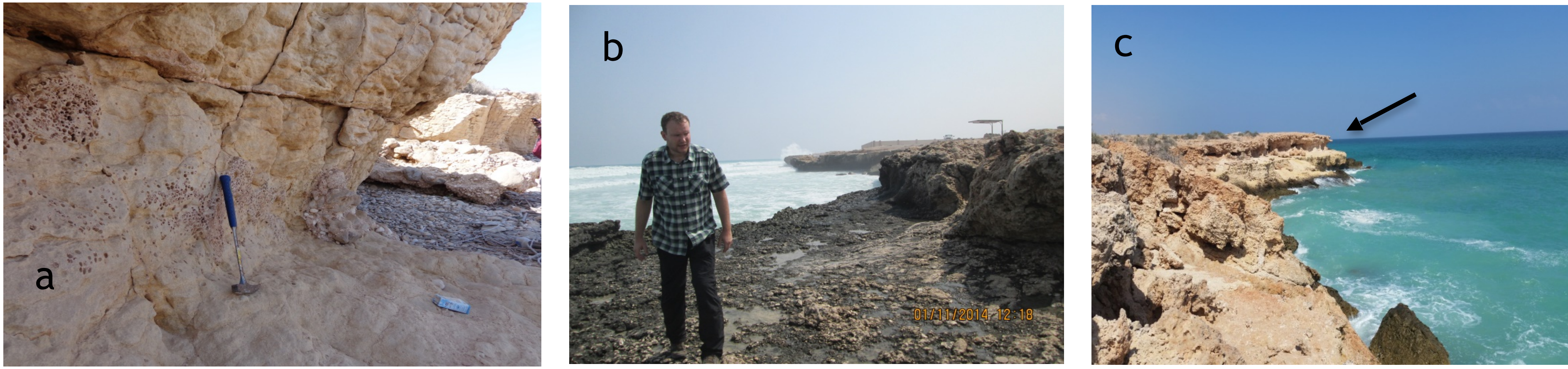

Figure 6S: Notches. a) Notch 1 with borings close to Tiwi, borings are preserved behind conglomerate b) Notch 1 close to Fins. c) Arrow shows notch 1 close to Dibbab

Figure 7S: Coral reefs a) Coral reefs near Fins, ~1.5m thick. B) Base of coral reef near Fins with contact to bored breeding ground c) Intensely bored breeding ground at the upper bedding surface of a bioclastic limestone. This breeding ground represents the base of the coral reefs.

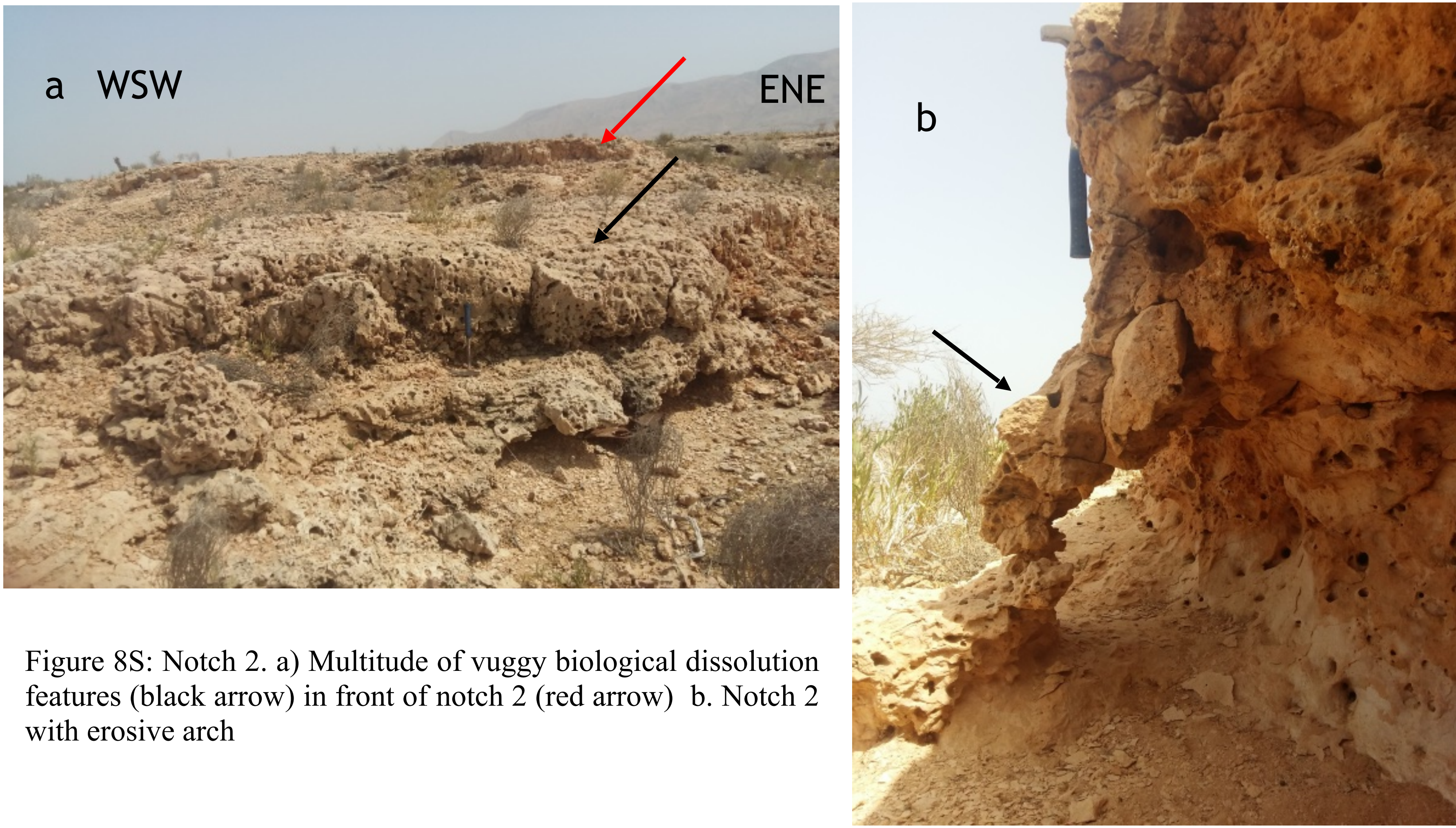

Figure 8S: Notch 2. a) Multitude of vuggy biological dissolution features (black arrow) in front of notch 2 (red arrow) b. Notch 2 with erosive arch

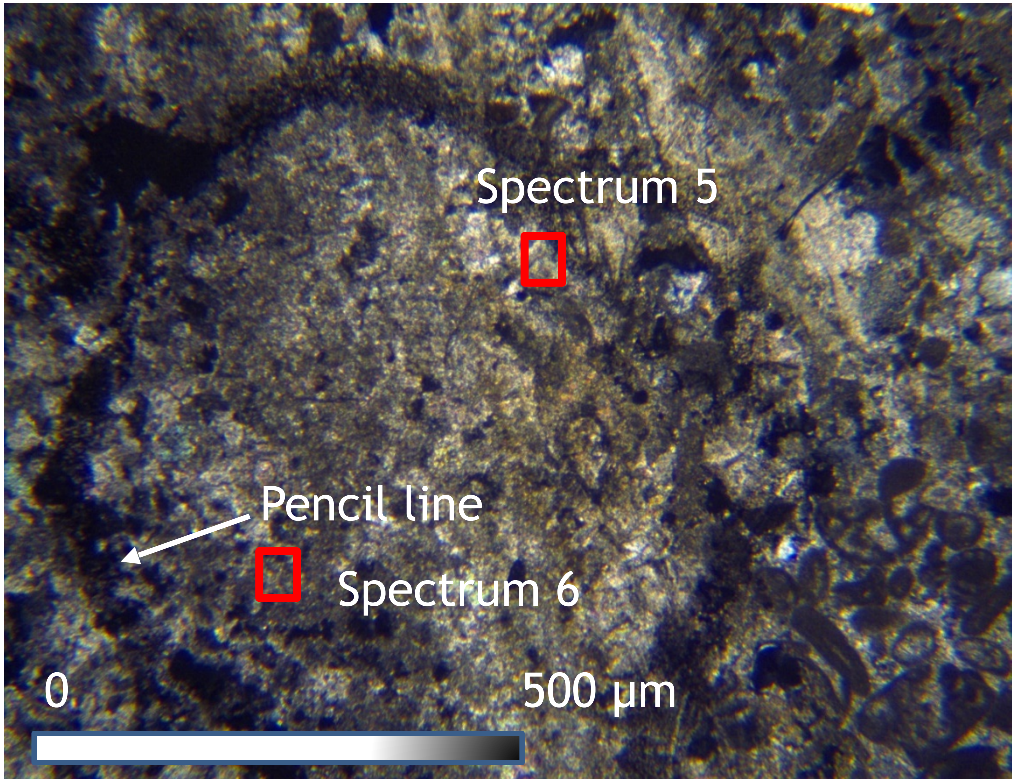

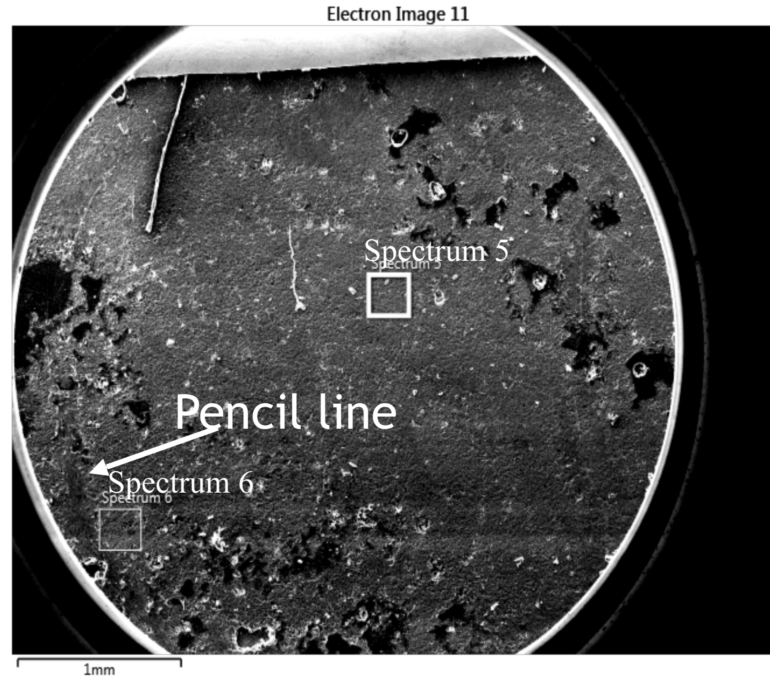

Sparite-Cement-spectra 5	Ca: 48.1 ±0.6%	Mg: 1 ±0.1%
Microcrystalline-spectra 6	Ca: 34.3 ±0.5%	Mg: 13.2 ±0.3%

Fig. 9S: Sample FE8 a) Red boxes in the thin section show the areas of the chemical analyses b) SEM image with white boxes showing the same areas as above. Table below shows the analysis' results of the two spectra 5 and 6 for Mg and Ca.

Figure 10S: FE11-Terrace 2

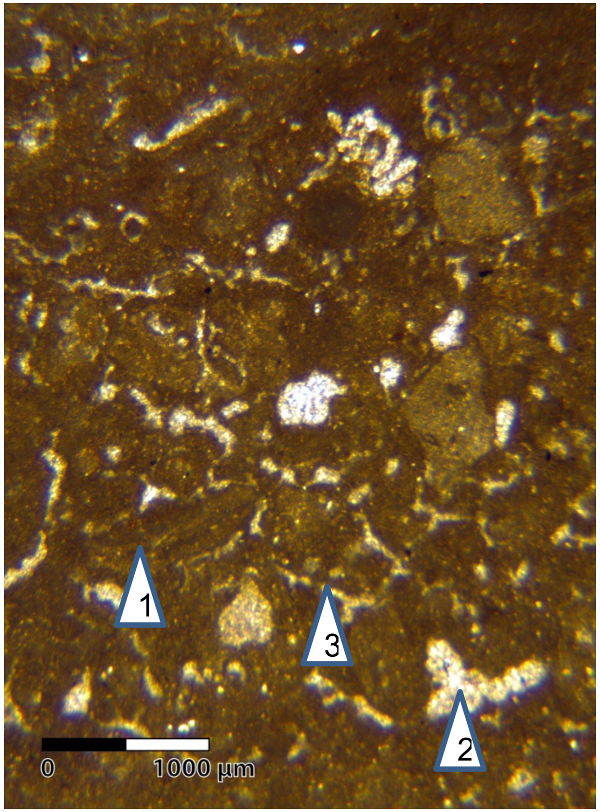

FE11: Pedogenic crust (arrow1) and calcite duricrust (arrow 2). Circumgranular laminae (arrow 3)

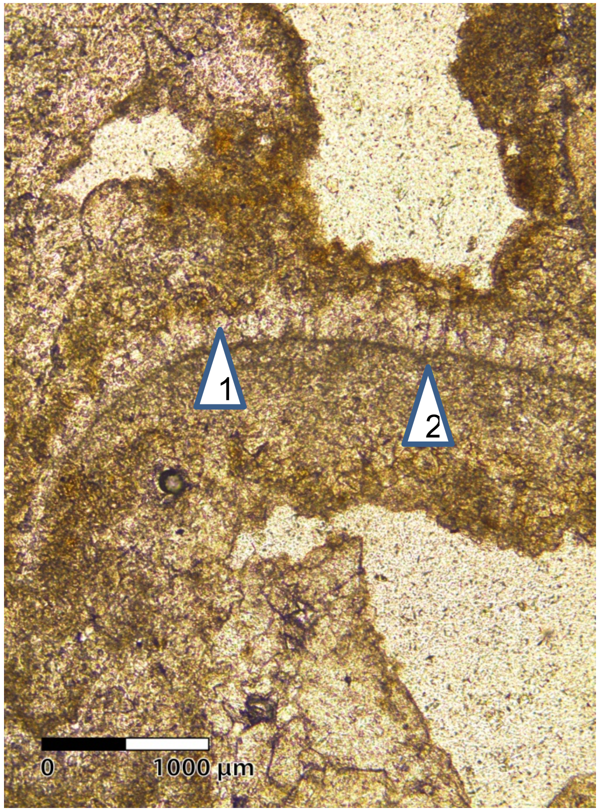

FE11: Isopachous equant cement and dark rim of microcrystalline cement (arrow 2)

Figure 11S: FE11-terrace 2

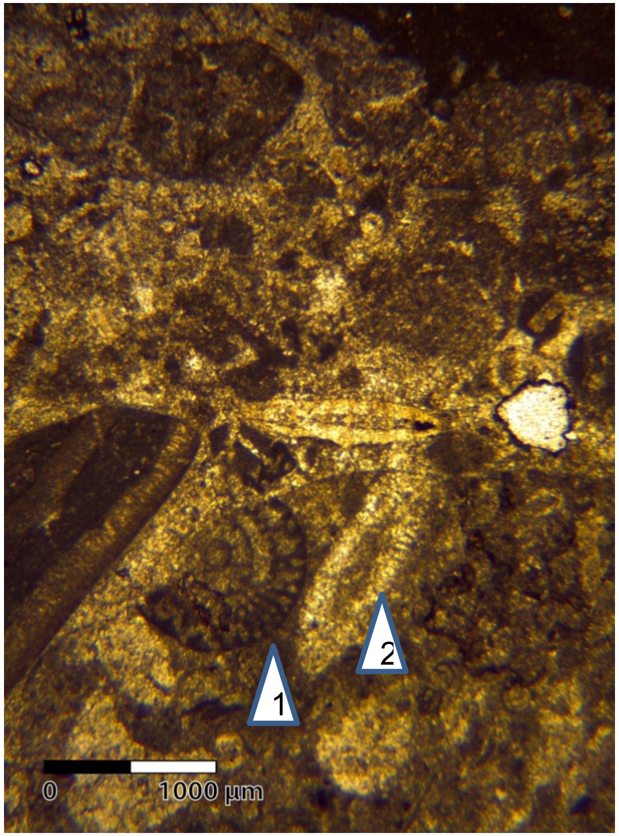

FE11: Bioclasitic conglomerate (arrow 1: benthic foraminifera, arrow 2: green algae)

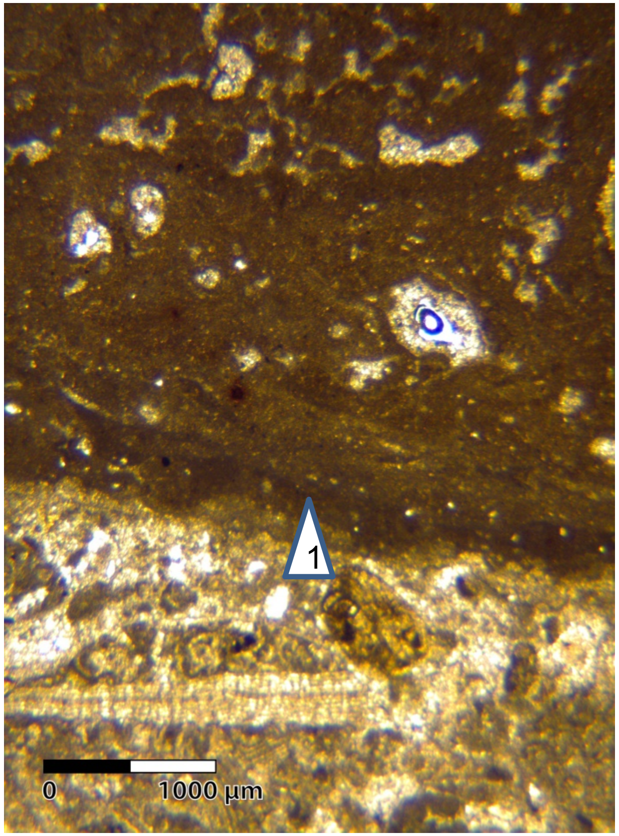

FE11:Pedogenic crust (arrow 1)

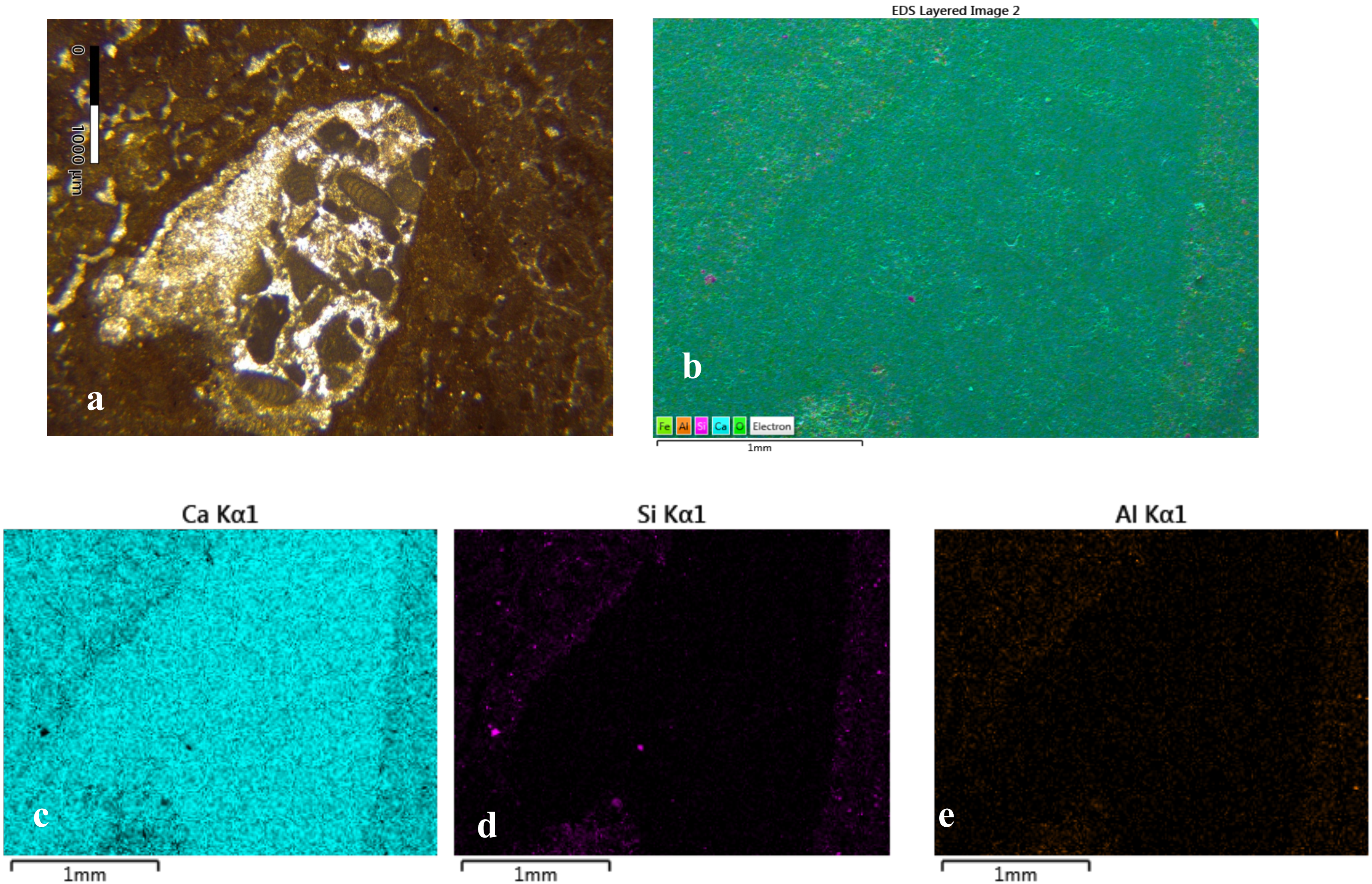

Figure 12S: Sample FE11. a) Clastic material within the pedogenic matrix. b) Map of the average chemical analysis, c) Map with Ca content, d) Map with Si content, e) Map with Al content. Brighter areas depict higher concentration of the respective elements.

Figure 13S: FE8-Terrace 2

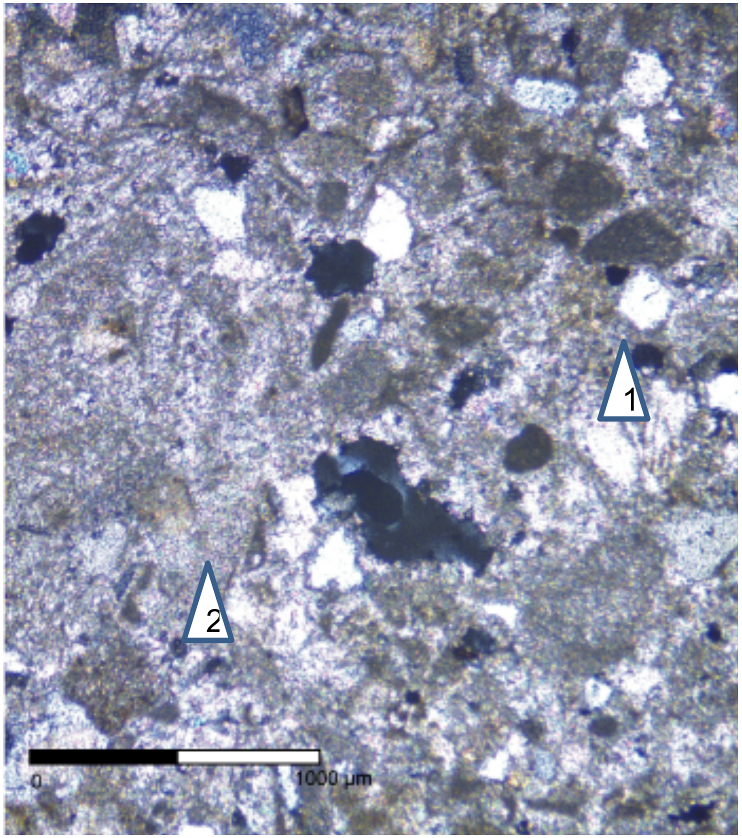

FE8: Quartz grains (arrow 1) and abundant microsparite (arrow 2).

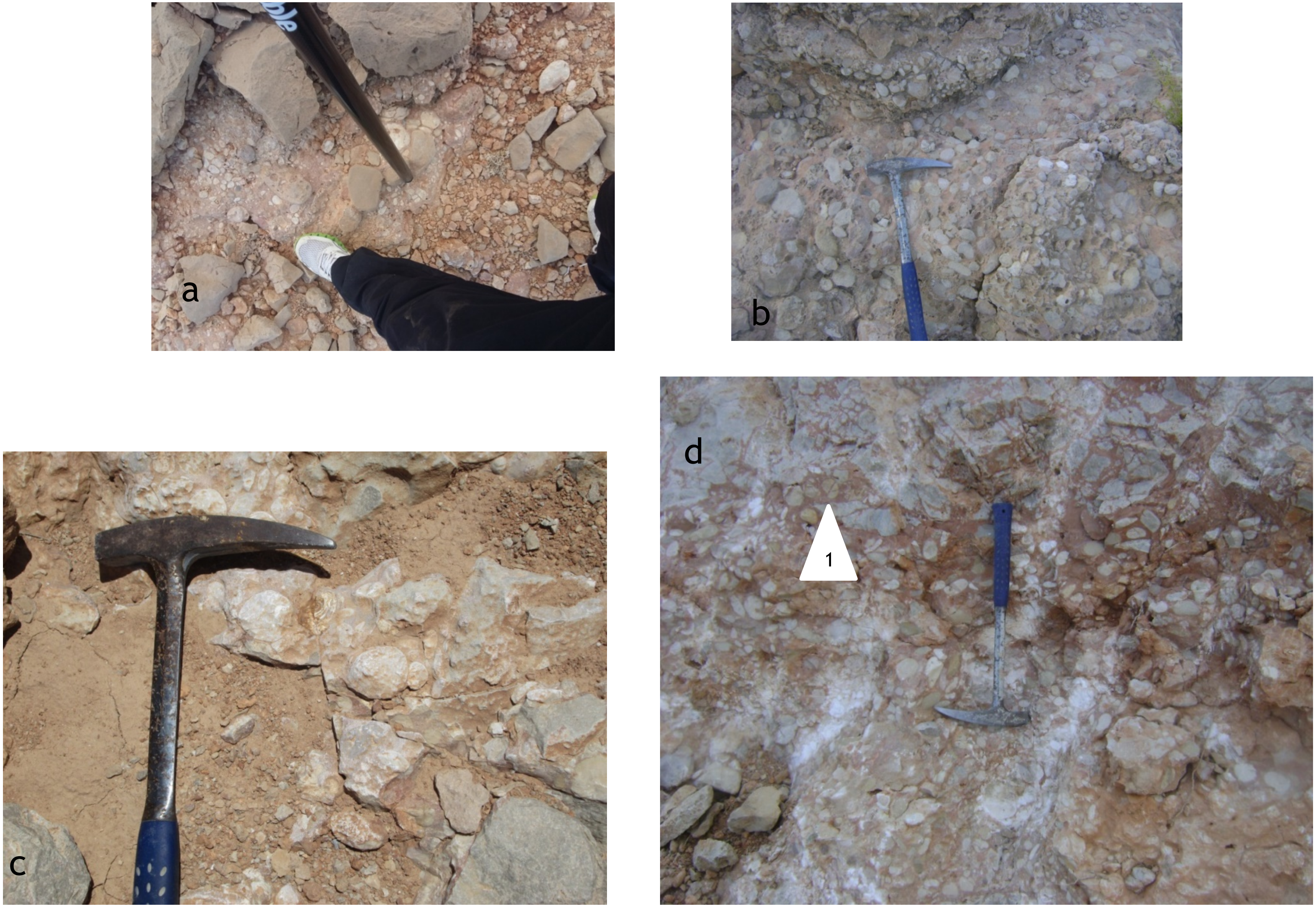

Figure 14S: Pedogenic red crust associated with the marine conglomerates of terrace 3 (a, b) in crack along a fresh road cut in the slope between terrace 2 and terrace 3 (c,d). Arrow 1 is pointing to displacive cement which offsets fragments of the same clast of the conglomerate.

Figure 15S: FE6-In the slope between terrace 2 to 3

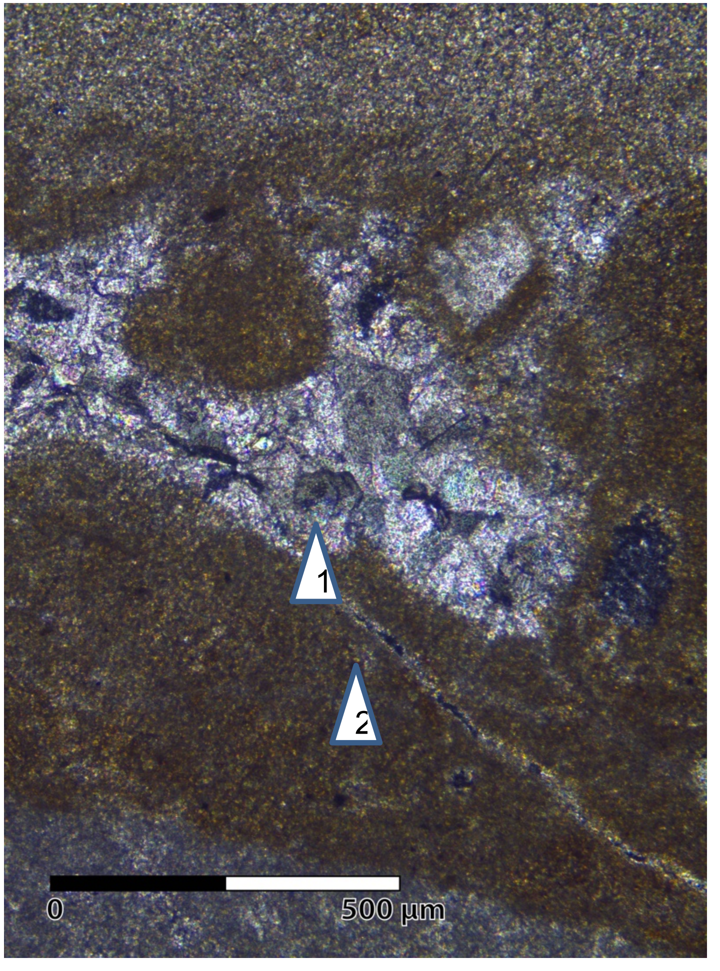

FE6: equant to drusy cement filling cavities (arrow 1) surrounded by pedogenic crust, (arrow 2)

Figure 16S: FE6-In the slope between terrace 2 to 3

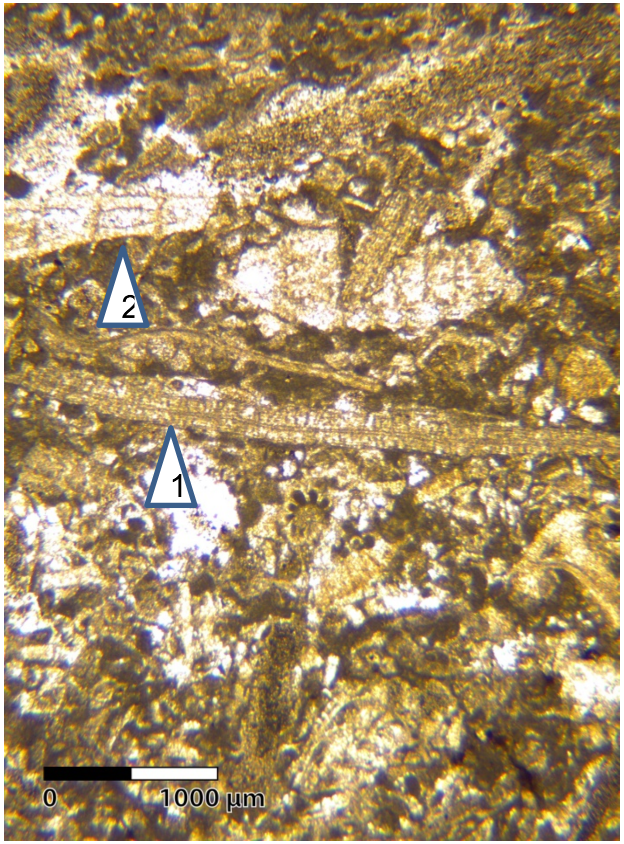

FE6: benthic foraminifera (arrow 1: *Discocyclina*, arrow 2: *Assilina*)

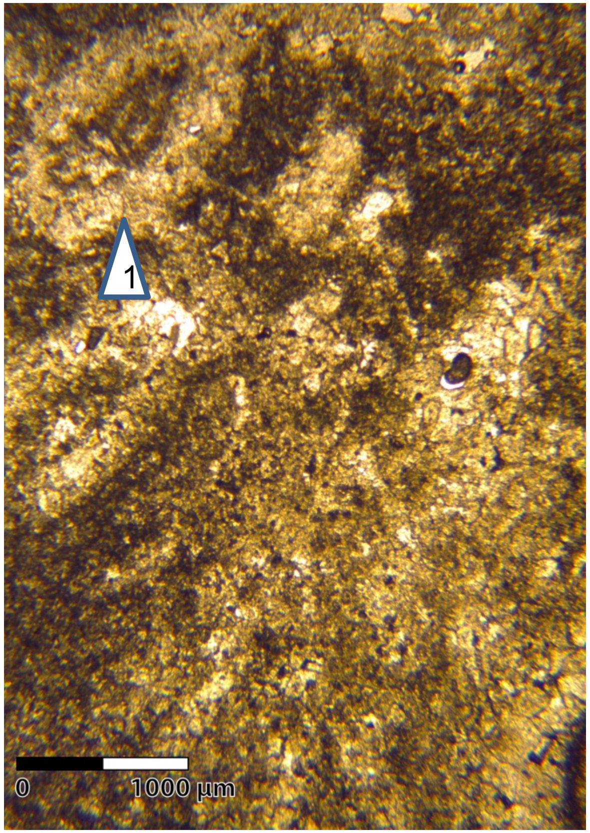

FE6:dolomite mimic replacement of green algae (arrow 1)

Figure 17S: FE13-Terrace 1

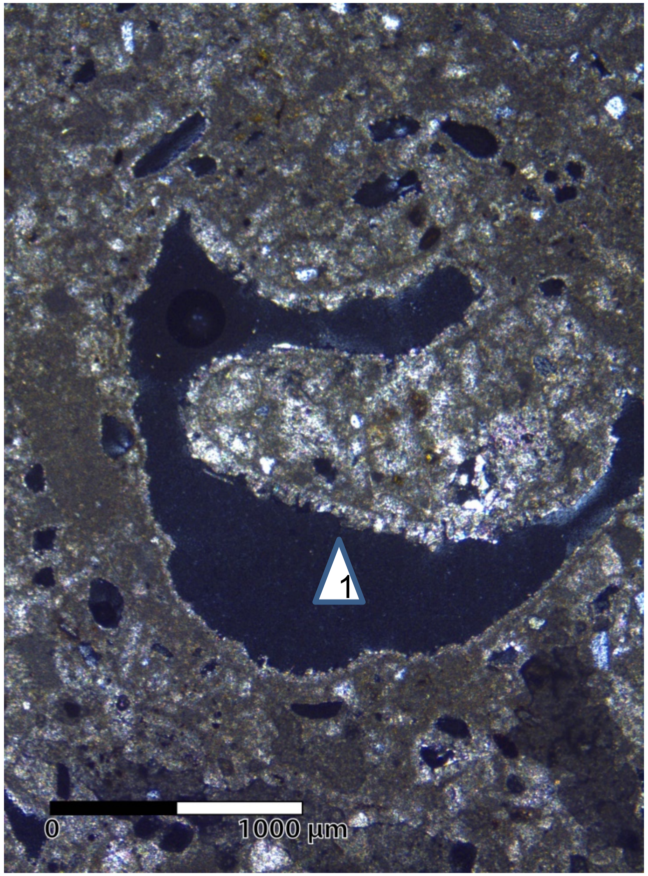

FE13: Bladed cement (arrow 1)

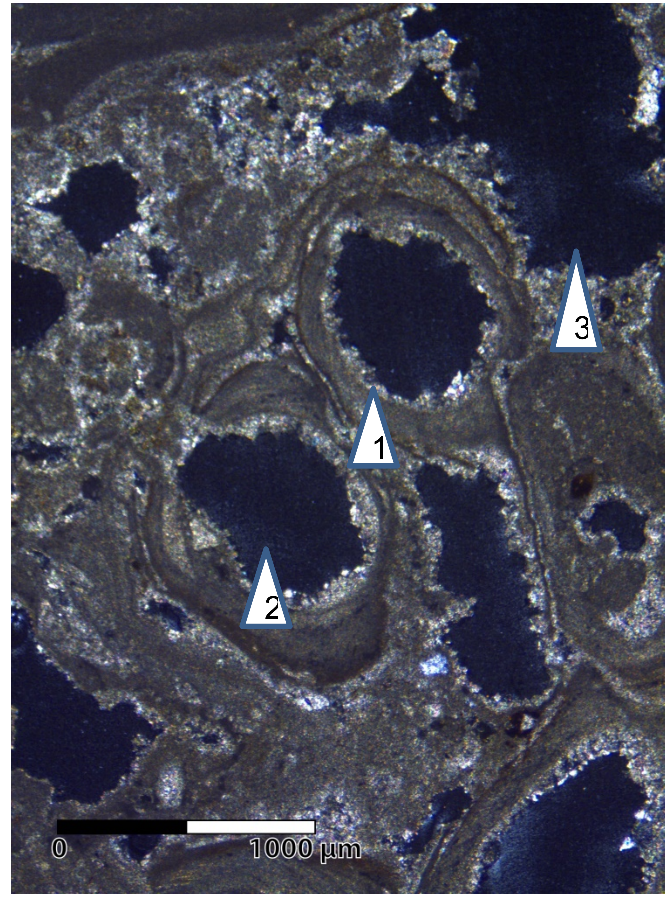

FE13: Dog tooth cement (arrow 1), moldic porosity (arrow 2), vuggy porosity (arrow 3)

Figure 18S: Samples FE13, FE5- terrace 1

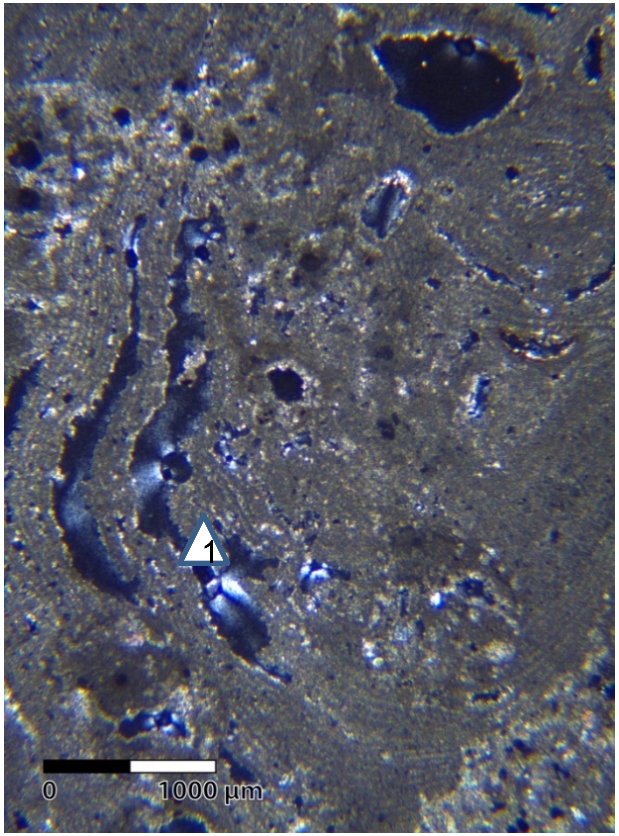

FE13: Red algae boundstone (arrow 1)

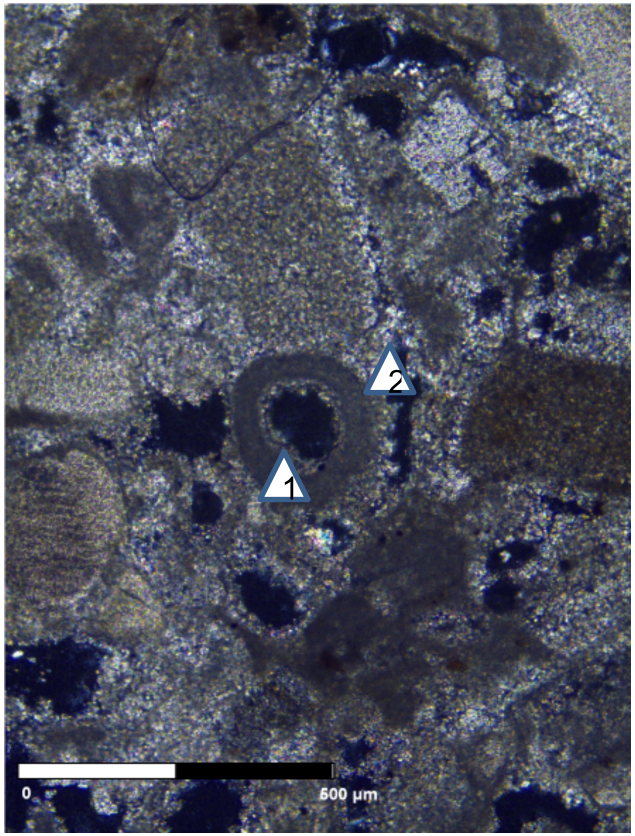

FE5: Moldic and vuggy porosity, isopachous microcrystalline cement (arrow 1) and equant cement (arrow 2)

Figure 19S: Sample N2b-terrace 1

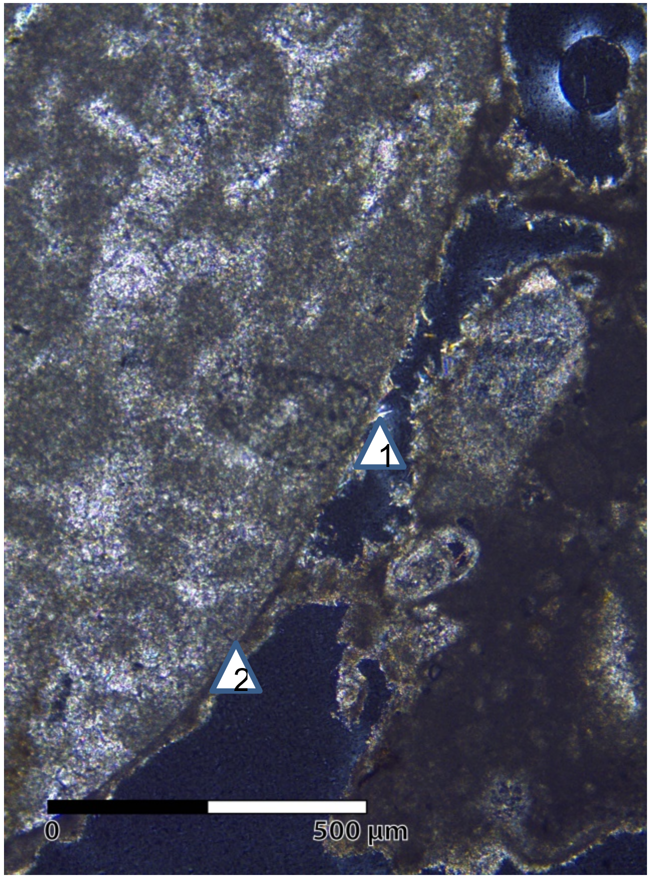

N2b: Acicular cement (aragonitic) between two clasts (arrow 1) following an earlier dark rim of microcrystalline calcite (arrow 2)

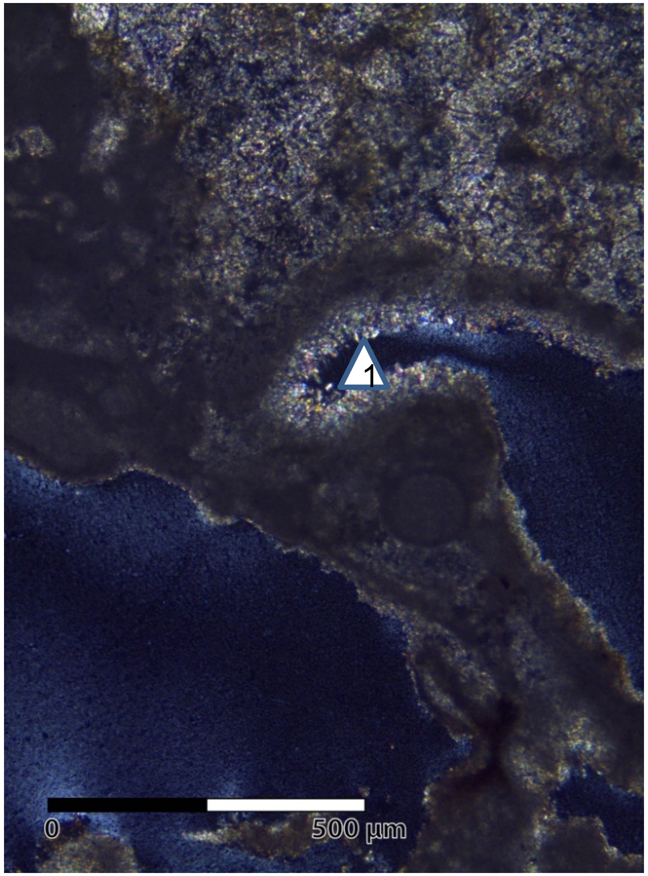

N2b: Acicular cement (aragonitic) lining clasts. The dark rim of microcrystalline calcite is also observed (arrow 1)

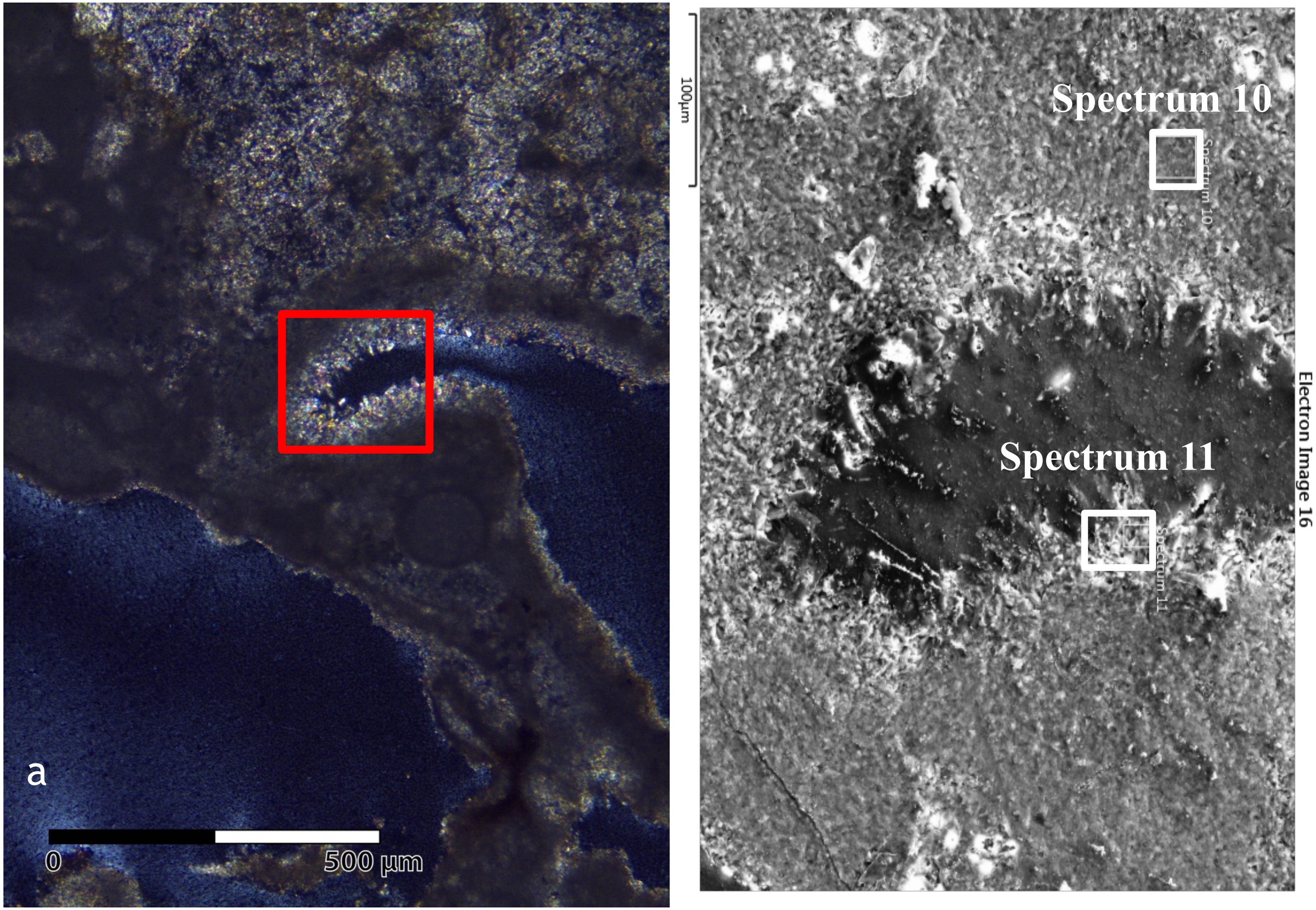

Matrix- spectrum 10	Ca:43.1 ±0.5	Mg: 4.5 ±0.1
Cement-spectrum 11	Ca:48.1 ±0.4	Mg: - not detected

Figure 20S: Sample N2b a) Red box in the thin section shows the area of analyses in b) SEM image and areas of chemical analyses (spectra 10 and 11). Table below shows the analysis' results of the two spectra 10 and 11 for Ca and Mg.

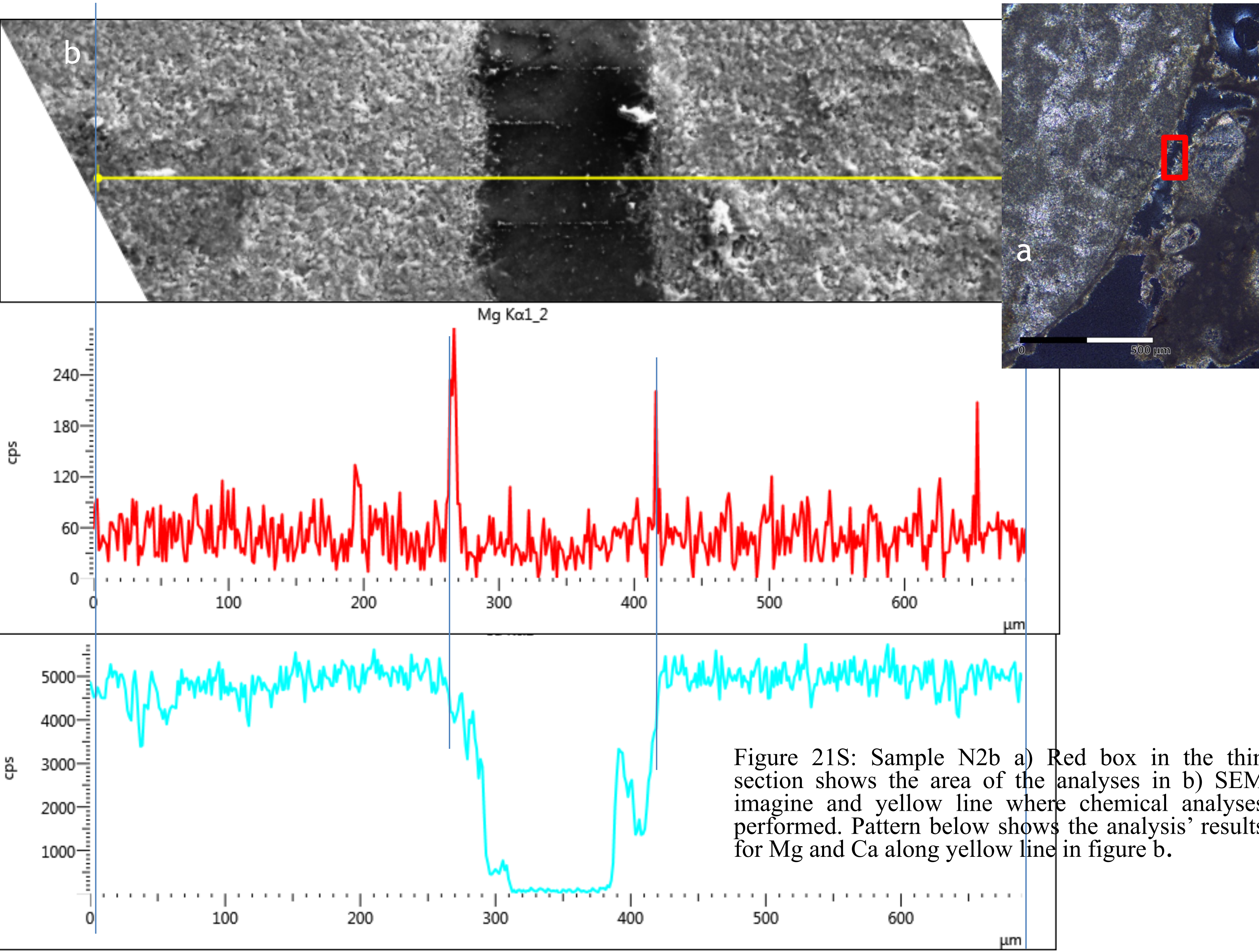

Figure 21S: Sample N2b a) Red box in the thin section shows the area of the analyses in b) SEM imagine and yellow line where chemical analyses performed. Pattern below shows the analysis' results for Mg and Ca along yellow line in figure b.

Figure 22S: Sample N2a, FE7-Notch 1

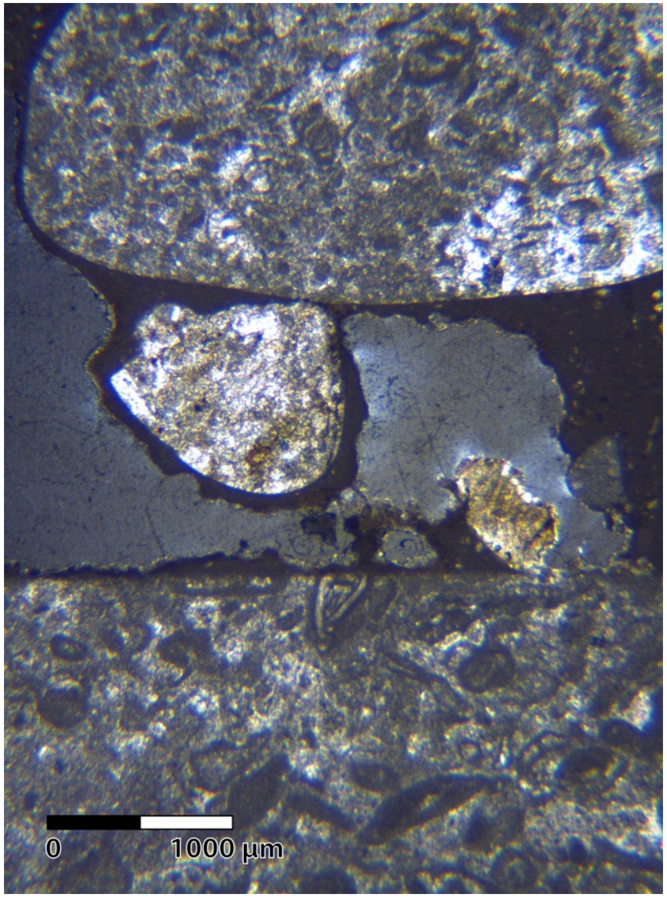

N2a: Vuggy porosity, in a poorly sorted and clast supported conglomerate

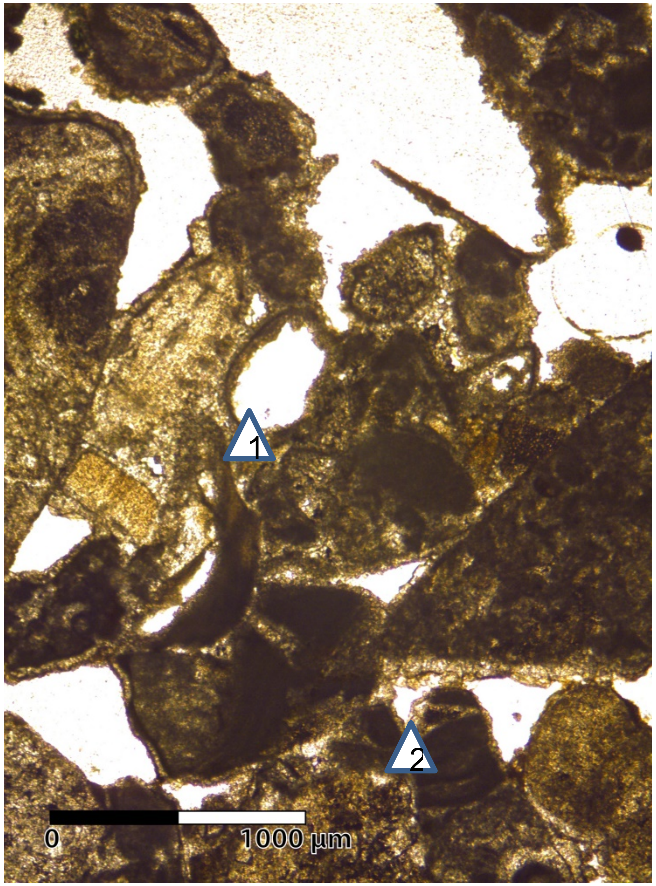

FE7: Microcrystalline rim cement lining a moldic pore (arrow 1) and bladed to equant cement (arrow 2)

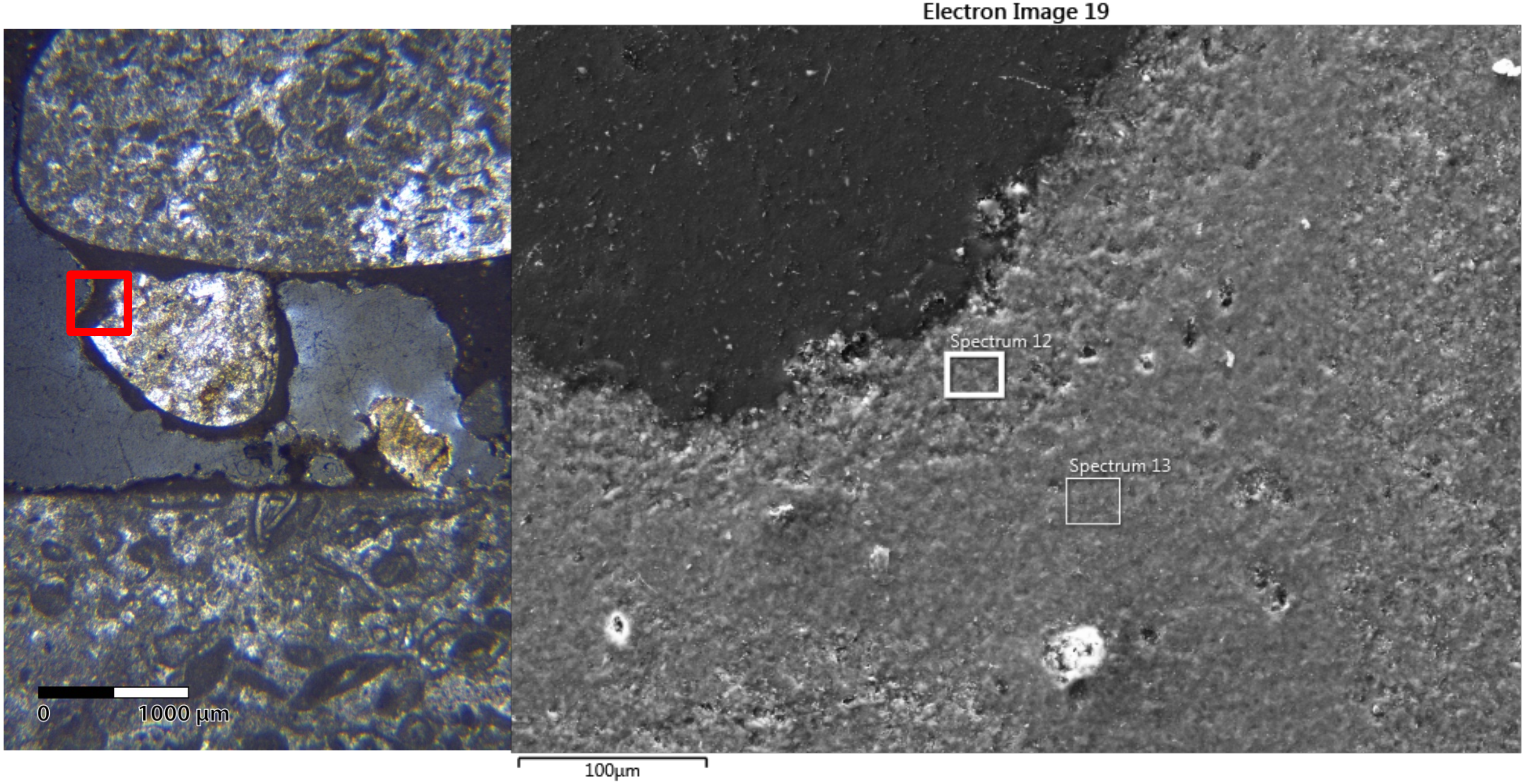

Matrix- spectrum 13	**Ca: 48.1 ±0.4%**	**Mg: 1.4 ±0.1%**
Cement-spectrum 12	Ca: 40.7 ±0.4%	Mg: 2.8 ±0.1%

Figure 23S: Sample N2a a) Red box in the thin section shows the area of analysis in b) SEM image and areas of chemical analyses (spectra 12 and 13). Table below shows the chemical analysis' results of the two spectra 12 and 13 for Ca and Mg.

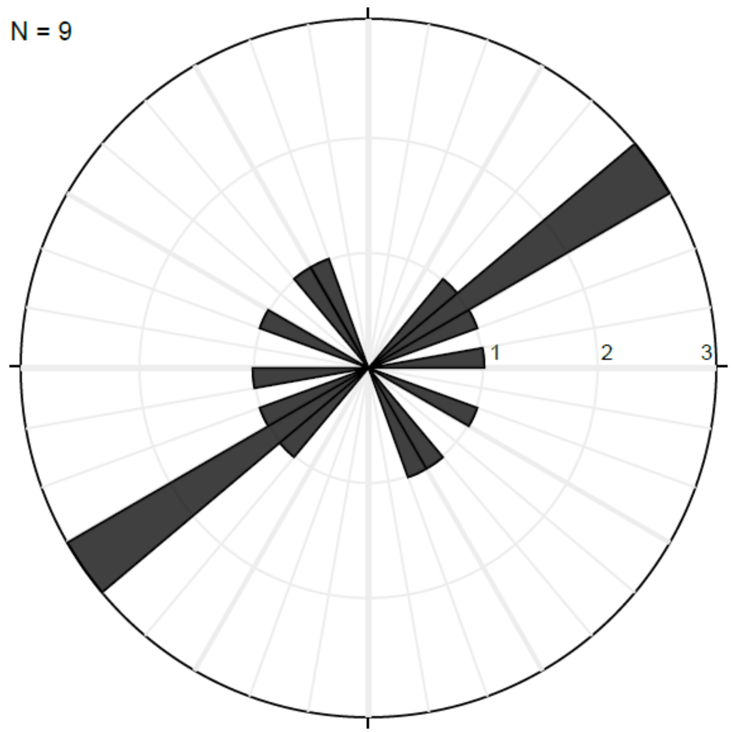

Figure 24S. Rose diagram for 8 newly discovered and analyzed faults (this study) of the study area. Details are provided in Tab. 1S. Fault 9 in table 1S is not considered "new".

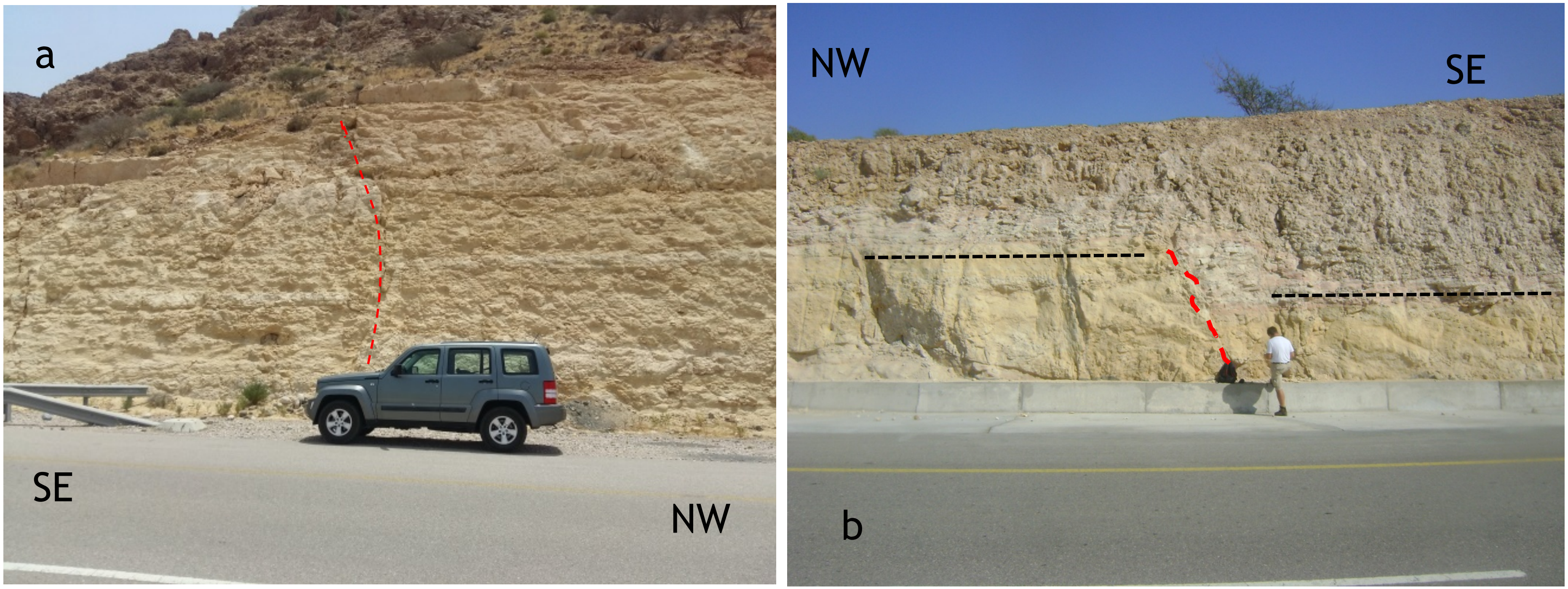

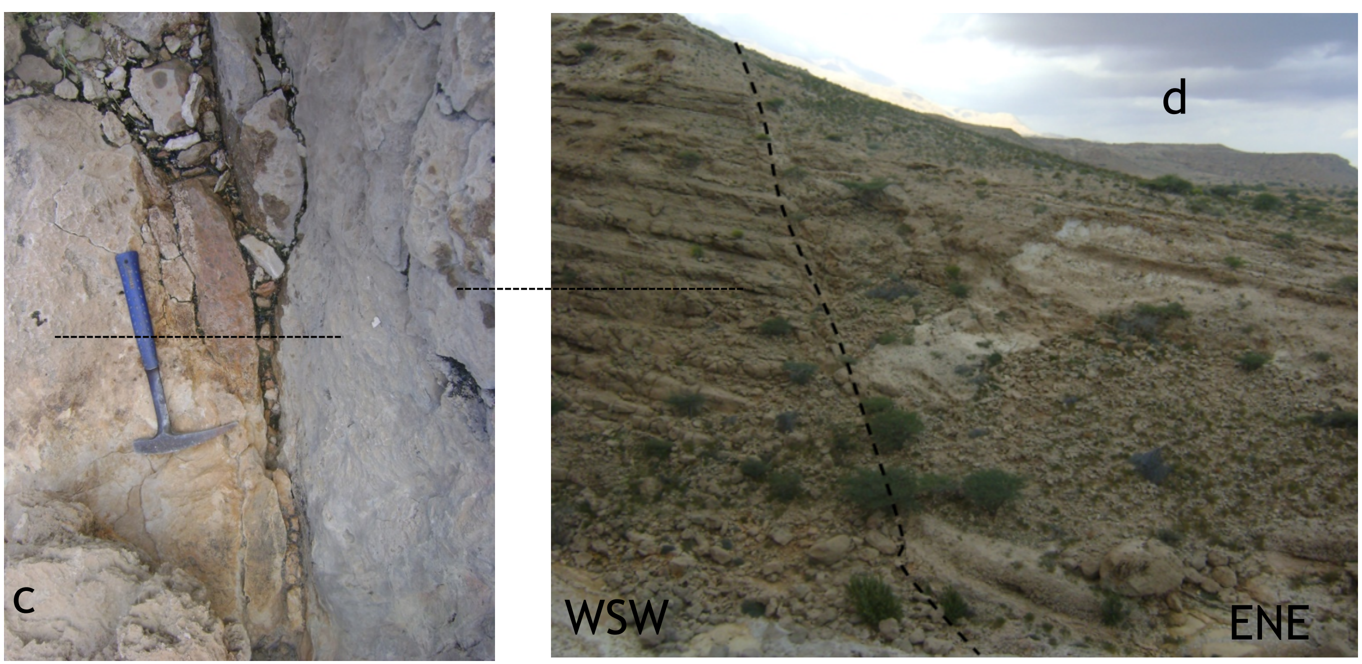

Figure 25S: a, b) Faults running almost perendicular to the coastline. Roadcut along the highway in the area between Dibbab and Fins c,d) Fault 8 and cataclastic texture in fault 8

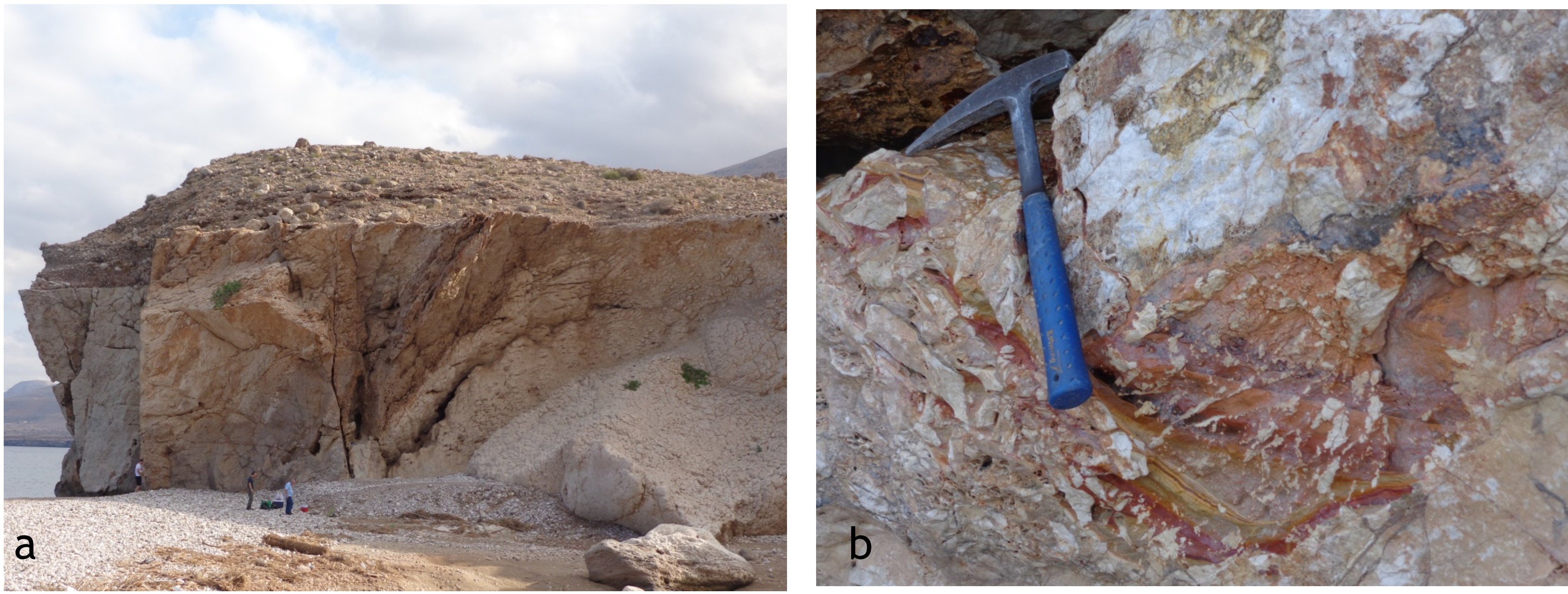

Figure 26S: a) Strike slip fault with positive flower structure (fault 9) b) tectonic breccia of fault 9

Figure 27S:
a) Sea flooded wadis between Muscat to Quriyat and b) Characteristic coastal wetlands with mangroves development

Table 1S. a) Tidal fluctuation on 28th November 2015, b) Tidal fluctuation on 31st October 2015

Muscat, Oman				a)
23.6167° N, 58.6000° E				
2015-11-28 Sat 4:58 AM GST 1.43 meters Low Tide				
2015-11-28 Sat 6:28 AM GST Sunrise				
2015-11-28 Sat 10:19 AM GST 2.62 meters High Tide				
2015-11-28 Sat 5:01 PM GST 0.29 meters Low Tide				
2015-11-28 Sat 5:18 PM GST Sunset				

Muscat, Oman				b)
23.6167° N, 58.6000° E				
2015-10-31 Sat 12:14 AM GST 2.89 meters High Tide				
2015-10-31 Sat 5:58 AM GST 1.43 meters Low Tide				
2015-10-31 Sat 6:10 AM GST Sunrise				
2015-10-31 Sat 11:22 AM GST 2.59 meters High Tide				
2015-10-31 Sat 5:27 PM GST Sunset				
2015-10-31 Sat 6:06 PM GST 0.48 meters Low Tide				

Table 2S. Faults identified in the area between Tiwi and Fins

	N	E	Dipping direction (degrees)	Dipping angle (degrees)
Fault1	23.07584	59.04775	144	62
Fault2	23.07329	59.04906	156	80
Fault3	23.06579	59.05477	140	62
Fault4	23.0671	59.05329	170	57
Fault5	23.07101	59.05072	318	75
Fault6	23.06771	59.05315	140	60
Fault7	23.06579	59.05477	204	89
Fault8	22.98422	59.12699	28	86
Fault 9	22.78222	59.28186	244	77

Table 3S. a) Age data, eustatic sea level, 2σ ±BP and ± mm/year as it was given in the references used for Fig. 9b

Table 1

Point number in Map 8	Reference	Elevation	Age BP	± BP	Eustatic sea level	Uplift mm/year	± mm/year	Method
1	Ridley and Seeley 1977	2.8	3812	145	-1	1.00		Carbon-14
2	McClure and Vita-Finzi 1982	1	4585	60	-1	0.44		Carbon-14
3	McClure and Vita-Finzi 1983	1.8	3695	50	-1	0.76		Carbon-14
4	McClure and Vita-Finzi 1984	2	4460	60	-1	0.67		Carbon-14
5	McClure and Vita-Finzi 1985	1.2	6020	50	-1	0.37		Carbon-14
6	McClure and Vita-Finzi 1986	3	4205	80	-1	0.95		Carbon-14
7	Wood et al. 2012	3.57	3320	30	-1	1.38	0.10	Carbon-14
8	Wood et al. 2012	3.61	3432	30	-1	1.34	0.10	Carbon-14
9	Wood et al. 2012	3.88	3422	25	-1	1.43	0.10	Carbon-14
10	Wood et al. 2012	4.04	4097	33	-1	1.23	0.10	Carbon-14
11	Wood et al. 2012	4.16	5548	27	-1	0.93	0.10	Carbon-14
12	Wood et al. 2012	3.90	30300	3500	-86	2.97	0.20	OSL

Supplementary part B
Thin sections description

- **Notch 1**

  – Sample N2a

The sample is a monomictic carbonate conglomerate (lithoclastic rudstone), poorly to moderately sorted and clast-supported. The clasts are bioclastic packstones with alveolinids, miliolids, nummulitids, orbitolites and a few peloids. The clasts derive from the Jifnayn Formation. The matrix is carbonatic-micritic with small fragments of undetermined clasts. There are mainly moldic and vuggy pores. Dissolution features cut through clasts and matrix. Pores are lined with microcrystalline cement.

  – Sample FE7

The sample is a polymictic grainstone to rudstone. Clasts include large crystalline dolostones and peloid/foraminiferal grainstones. Nummulitids are common in the clasts. The origin of the peloid/foraminferal clasts is likely the Jifnayn Formation. The clasts form a support structure. The grains are cemented together, and some clasts have been dissolved (vuggy pores; commonly dissolved cortoids), also parts of the matrix. The pores are lined by thin isopachous rim cement. The cement is microcrystalline transitional to equant and to bladed cement and may evolve into a drusy cement.

- **Terrace 1**

  – Sample N2b

The sample is a monomictic carbonate conglomerate (lithoclastic rudstone), moderately to well sorted and clast-supported. The clasts include alveolinids, miliolids, nummulitids, orbitolites, bryozoans, fragments of large mollusks, sponges, red algae, boundstones, and peloids. The clasts also stem from the Jifnayn Formation. The matrix is carbonatic-micritic with small fragments of undetermined clasts, red algae, gastropods, possibly with some ostracod shells and discorbids(?). There are mainly moldic and vuggy pores which are lined by microcrystalline cement (first generation cement), followed by a cement of a mesh of aragonite needles. The aragonite needles are preserved in well-protected parts of pores.

  – FE13

The sample is a red algae boundstone. The matrix is a packstone with red algal fragments, small peloids and angular fine sand-sized quartz grains. Besides partly primary growth framework pores, there are vuggy pores and molds of gastropods and other allochems. The cement is of the microcrystalline and/or bladed and/or dog tooth type.

  – FE5

Bioclastic grainstone with foraminiferas (nummulites, miliolids, and others), bivalve clasts, echinoderm fragments, red and green algae. There are abundant micritised grains, some are dissolved from the inside. Vuggy pores dominate, but there is also some moldic porositry. The pores are lined with thin isopachous, microcrystalline calcite. The clastic material consists of angular quartz sand dispersed in the sample (5%).

- **Terrace T2**
  - FE11

The large sample is divided into two parts. The lower part is a polymictic, lithoclastic rudstone/conglomerate. The matrix of the large clasts is a bioclastic grainstone with fragments of red algae, some hyaline, evolute foraminifera like operculina(?), fragments of alveolinids. The pores are mainly vuggy, and the cement consists of micritic cement lining the clasts, followed by isopachous cement, followed by equant sparite as the main cement. The rudstone is overlain at an erosive contact by a pedogenic crust, consisting of a lower segment with dark, micritic, undulated laminae, followed upward by circumgranular cracks and possibly nodular caliche. There are no open pores. Calcite equant cement is characterizing the duricrust.

  - FE8

The sample is a rudstone with pebble size dolomite (crystalline dolomite), foraminiferal packstone and peloid grainstones (with 7 to 8% quartz sand) and biomudstone to biowackstone. The clasts are embedded in a matrix of 5 to 10% quartz sand, foraminifera, bivalves debris, peloids, cortoids bound together by microsparite. Moldic or vuggy pores are poorly lined with a thin microcrystalline calcite and also some bladed cement. Again, marginally micritized grains are dissolved from the inside.

- **Terrace T2 to terrace T3 cracks**
  - Sample FE6

The sample is an oligomictic rudstone with three pebble-sized clasts. The first clast is foraminiferal micrite (mudstone to wackestone) with nummulitids and triserial foraminiferans, orbitolites and echinoderm debris. The second clast is a foraminiferal grainstone with bryozoans, nummulitids (*Assilina*),*Discocyclina,* echinoid and bryozoan debris. The third clast is a strongly recrystallized algae packstone with crystalline fabric (dolostone?) with mimic replacement of green algae. The matrix is pedogenic micrite, with components of reworked pedogenic crust and small lithoclasts, also crystals of rhomb shape crystals (dolomite). The matrix contains fracture pores. The cement is equant or drusy.

Description of Figure 1b from the manuscript text

The Upper Cretaceous (Maastrichtian) Al-Koud Formation is comprised of deltaic deposits and contain mainly cherts and ophiolite fragments from the erosion of the Hawasina and ophiolite nappes (Wyns et al. 1992a), respectively. After deposition of the Al-Koud Formation the study area was below the sea level (relatively tectonically inactive period) for a long time. The respective formations in our study area are mainly the Jafnayn, Rusayl, Abat, Seeb and Shama formations with ages ranging from the upper Paleocene to upper Oligocene (Roger et al. 1991, Wyns et al. 1992b). The Jafnayn, Rusayl and Abat formations are comprised of marine limestone and marly limestone. The Seeb Formation consists of massive bioclastic limestone with subordinate shale and sandstone. The Shama Formation consists of massive bioclastic limestone of reefal to outer shelf limestone (Roger et al. 1991). The Tahwah, Sur and Salmiyah formations which are exposed mainly in Sur (they are not shown in Fig. 1b because they are outside the study area) are the youngest Neogene rocks, and they are mainly represented by coarser clastic sediments (Wyns et al. 1992a). In any case, our study area between Fins and Tiwi was exposed to erosion from the Oligocene to early Miocene and supplied detritus as littoral drift towards the Sur and possibly Quriyat depressions. Quaternary deposits cover the most recent marine terraces close to the coastline and they are presented in Fig. 1b (Wyns et al. 1992a)

Analysis of the term “equivalent” terrace between Tiwi and Fins

The term “equivalent” is used for the terraces of analogous relative position, and similar lithological characteristics of the conglomerates found in the respective terraces For example, sample FE6 represents depositional environment strongly influenced by pedogenic processes (Fig. 7b), and the same characteristics have been identified in several areas in the seaward slopes and at the top of the terrace T3 (sample FE6 in Fig. 7b and Fig 9Sa-d in the supplementary information). Thus, terrace T3 and the pedogenic crust identified (Fig. 5Sc in the supplementary information), is the “reference” terrace.